Available online at www.sciencedirect.com
ScienceDirect
Journal of Colloid and Interface Science 317 (2008) 458–468
JOURNAL OF Colloid and Interface Science
www.elsevier.com/locate/jcis

Mechanism of nanocapsules formation by the emulsion–diffusion process

Delphine Moinard-Chécot [a], Yves Chevalier [a,*], Stéphanie Briançon [a], Laurent Beney [b], Hatem Fessi [a]

[a] *Laboratoire d'Automatique et de Génie des Procédés, LAGEP, UMR 5007 CNRS, Université Claude Bernard Lyon 1, ESCPE Lyon, 43 Bd 11 Novembre 1918, 69622 Villeurbanne Cedex, France*

[b] *Laboratoire de Génie des Procédés Microbiologiques et Alimentaires, GPMA, EA 1684, ENSBANA, Université de Bourgogne, 1 Esplanade Érasme, 21000 Dijon, France*

Received 12 July 2007; accepted 29 September 2007

Available online 3 October 2007

Abstract

A detailed investigation into the mechanisms of nanocapsule formation by means of the two stages "emulsion–diffusion" process is reported. Such widely used process is still poorly understood. An emulsion of oil, polymer and ethyl acetate is fabricated as a first step; dilution with pure water allows ethyl acetate to diffuse out from the droplets, leaving a suspension of nanocapsules at the end. It has been shown that the size of nanocapsules was related to the chemical composition of the organic phase and the size of primary emulsion through a simple geometrical relationship. As a consequence, most of the properties of the nanocapsules were decided at the emulsification step. The influence of several formulation and processing parameters of the primary emulsion was studied accordingly. The thin polymer membrane of nanocapsules was observed by means of cryo-fracture electron microscopy. Finally two experiments were designed for a mechanistic investigation of the diffusion step. A step-by-step diffusion of the organic solvent takes place by successive partition equilibria of ethyl acetate between the droplets and aqueous phase. A time-resolved experiment shows the fast diffusion (less than 20 ms) related to the small droplet size of the emulsion.

Keywords: Nanocapsule; Emulsion; Process; Emulsion–diffusion; Polycaprolactone

1. Introduction

Aqueous suspensions of biodegradable polymer nanoparticles are very attractive carriers for drug delivery because of their versatility for their formulation in pharmaceutical dosage forms [1–4]. Particles of submicronic size required for parenteral administration and are also favorable for a fast penetration across biological membranes. The term nanoparticle is used to define solid colloidal particles having sizes (diameters) ranging from 10 to 1000 nm and to describe both nanospheres and nanocapsules. Nanocapsules consist in a liquid core surrounded by a polymeric membrane; their internal structure is of the "core–shell" type. The active substance is solubilized in the oil core. In this contribution, we focus on biodegradable nanocapsules of poly(ε-caprolactone) prepared by the "emulsion–diffusion" process. This later technique presents clear advantages compared to the other existing methods such as the use of pharmaceutically acceptable organic solvents, high yields of encapsulation, high reproducibility, better control of the particle size and easy scaling-up. The "emulsion–diffusion" method summarized in Fig. 1 was first proposed by Quintanar-Guerrero et al. [5–8]. It is a two-step process based on a conventional emulsification step followed by a removal of part of the oil phase as a second step. First, an oil-in-water emulsion is fabricated with "oil phase" containing the polymer and the oil in an organic solvent. The elimination of the organic solvent contained in the oil phase causes the separation of the polymer and the oil and a reduction of the particle size. Such removal of organic solvent is made by means of its diffusion into the aqueous phase caused by water addition (diffusion step); then the organic solvent can be safely evaporated under reduced pressure. The organic solvent is selected such that the oil and polymer are both soluble in it, and it is partly soluble in water for the diffusion by dilution to be possible. Ethyl acetate is an exam-

* Corresponding author. Fax: +33 4 72 43 16 82.
E-mail address: chevalier@lagep.univ-lyon1.fr (Y. Chevalier).

0021-9797/$ – see front matter
doi:10.1016/j.jcis.2007.09.081

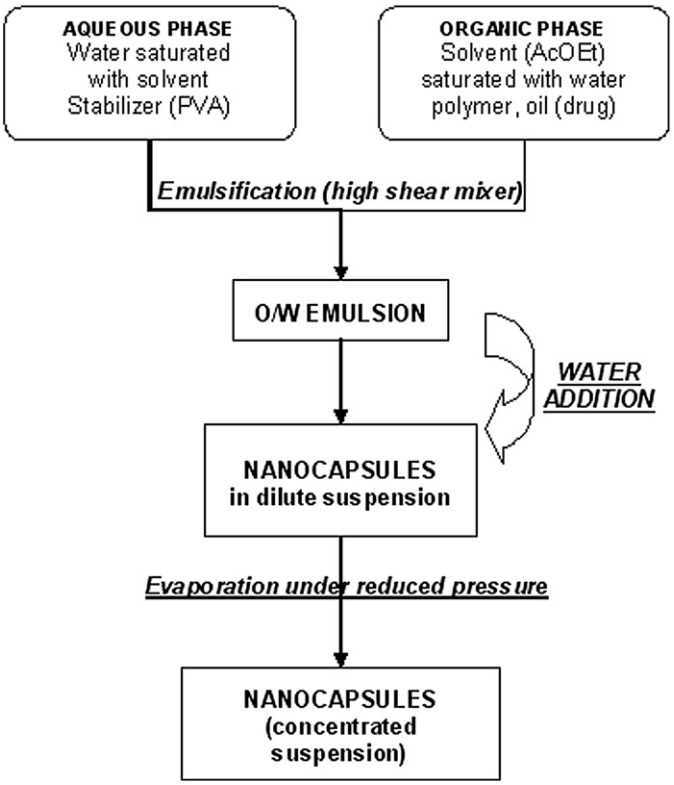

Fig. 1. Preparation of nanocapsules by the emulsion–diffusion process.

ple of such favorable solvent. Such diffusion process is milder than the direct evaporation of the organic solvent that is often performed in microencapsulation technology. Nanocapsules do not resist a direct evaporation of the solvent, possibly because of the mechanical stress when gas bubbles form inside the aqueous suspension. The formation of nanocapsules occurs at the diffusion step when the organic solvent goes out of the oil droplets, leaving the immiscible polymer and oil inside. More specifically, the organic phase is first made of polycaprolactone and oil dissolved in ethyl acetate (previously saturated with water) and the aqueous phase (previously saturated with ethyl acetate) contains the emulsifier (stabilizer). An oil-in-water emulsion is fabricated using a conventional emulsification technique; the subsequent addition of water to the system causes the solvent to diffuse from emulsion droplets, resulting in the formation of nanocapsules.

The aim of the present work is to get a better understanding of the nanocapsule preparation.

In particular, the diffusion step appears as a key-step that deserves more attention. However, technical difficulties coming from the small size of the particles and the fast rate of the diffusion step do not allow direct measurements. Therefore, we first showed the geometric relationship between the primary emulsion and the final nanocapsule sizes. The effects of formulation parameters on the nanocapsule final size were investigated. Experimental evidence of the presence of a polymer shell around the oil core was obtained from electron microscopy. Finally, the diffusion step has been studied at its intermediary stages and a time-resolved experiment using fast mixing in a stopped-flow instrument was attempted.

2. Experimental

2.1. Materials

The polymer used for the nanocapsule preparation was poly(ε-caprolactone), PCL (Sigma-Aldrich) with a weight-average molar mass of 80 000 g/mol. The oils Miglyol 812 (capric/caprylic triglyceride), Miglyol 829 (mixture of succinic triglycerides of fatty acids caprylic/capric) and Miglyol 840 (propylene glycol dicaprylate/dicaprate) were provided by Condea Chemie GmbH [9]. Ethyl acetate, AcOEt, from Aldrich was used as organic solvent. The stabilizer poly(vinyl alcohol), PVA, of molar mass 88 000 g/mol was purchased from Aldrich. Deionized water was used for the preparation and for the dilution of the emulsions.

2.2. Nanocapsule preparation

Nanocapsules were prepared by "emulsion diffusion" method described in Fig. 1. First, mutually saturated aqueous and organic phases were prepared. The saturated water contains 8.3% of ethyl acetate and the saturated solvent contained 3% of water [10]. PVA was dissolved in saturated water at 50 °C for 2 h. PCL was dissolved in saturated ethyl acetate at 50 °C during 2 h and oil was added when the solution has cooled back to room temperature. The resulting organic solution was poured into the aqueous phase and emulsified with a rotor–stator device Ultra-Turrax® T25 for 10 min. The oil-in-water emulsion (O/W) formed at room temperature. The dispersed droplets were converted into nanocapsules in the second step of solvent diffusion. The addition of a large volume of water (4 times the volume of the emulsion) to the emulsion under gentle stirring with a magnetic bar allowed the ethyl acetate to leave the droplets. The organic solvent and a part of the water were thereafter removed by evaporation under reduced pressure to afford a purified and concentrated suspension.

The type and content of the ingredient in the formulations have been varied along the study. A typical recipe is as follows: [PVA] = 2.5% w/w in aqueous phase (40 mL), [PCL] = 2% w/w and Miglyol 812 = 5% w/w in organic phase (10 mL). The emulsion was prepared by stirring with a Ultra-Turrax® T25 rotor–stator shearing device. The mix of aqueous and organic phases of 50 mL overall volume was contained in a 100 mL cylindrical beaker of 4.5 cm diameter and the S25N18G shaft of the Ultra-Turrax® T25 was dipped at a 2.5 cm depth out of the full 3.5 cm height of liquid. Mixing lasted 10 min at 8000 rpm. For the above example, the diameter of the final nanocapsules was 450 nm.

2.3. Characterization of nanocapsules

2.3.1. Size distribution

The particle size distribution was determined by light scattering measurements using a small-angle light scattering instrument Coulter® LS 230 (Beckman Coulter) or a dynamic light scattering instrument Malvern® Zetasiser 3000HS. Measurements were always made in triplicate. These two light scattering

techniques are complementary since they are sensitive to different size-ranges and they differ a lot in their basic principle. Thus small-angle light scattering is based of a measurement of the time-averaged scattered intensity as a function of the scattering angle; according to the explored angular domain, particle diameters are measured between 100 nm and 2 mm. Dynamic light scattering is a measurement of the Brownian motion of the particles that is related to their hydrodynamic diameter; the upper limit of the diameters that can be measured is 2 μm. A dilution of the suspension is required for both techniques. The dilution of nanocapsules was made with pure water, whereas the primary emulsion was diluted with its continuous phase, that is, water saturated with ethyl acetate. In small-angle light scattering measurements, the emulsions were diluted until the transmission was 88%, as recommended by the supplier for optimum operational conditions. The size distribution was calculated from the Mie theory according to the following optical model. The real part of refractive index of the particles was 1.45, close to that of Miglyol [11] and polycaprolactone, and the imaginary part was zero; the refractive index of water was 1.33. The suspensions were diluted to approximately 10^{-4} for dynamic light scattering, so that the count rate was of the order of 200 kHz. The size distribution was calculated from the auto-correlation signal using the CONTIN algorithm.

2.3.2. Morphological study

Electron microscopy techniques were used to assess the morphology of nanocapsules. Scanning Electron Microscopy, SEM, was performed with a Hitachi S800 FEG microscope at the "Centre Technologique des Microstructures" (CTμ) at the University of Lyon (Villeurbanne, France). A drop of diluted aqueous suspension of nanocapsule was deposited on a flat steel holder and dried at room temperature. The sample was finally coated under vacuum by cathodic sputtering with gold and palladium (Technics, Balzers). The samples were observed by SEM under an accelerating voltage of 15 kV.

Transmission Electron Microscopy, TEM, was performed with a Topcon EM 002B microscope. A small drop of suspension was deposited of a microscope grid (copper support covered with carbon) and slowly dried in open air. The dry samples were observed by TEM under 200 kV acceleration voltage. Observations were made either directly on the aqueous suspensions diluted with water, or after negative staining with a 2% sodium phosphotungstic acid solution.

Freeze-fracture electron microscopy provided a mean of visualizing the interior of nanocapsules. The preparation of the freeze-fracture replicas were performed at the CTμ of the University of Lyon with a Balzers freeze-fracture unit. The diluted nanocapsule suspensions were frozen, and the frozen blocks were fractured with a knife blade. The resulting fracture faces were shadowed with platinum sputtering at 45° incidence followed by carbon deposition at 90°. The samples were then dissolved away from the replicas, the platinum on carbon replicas were floated off, put on the supporting grid and observed in TEM.

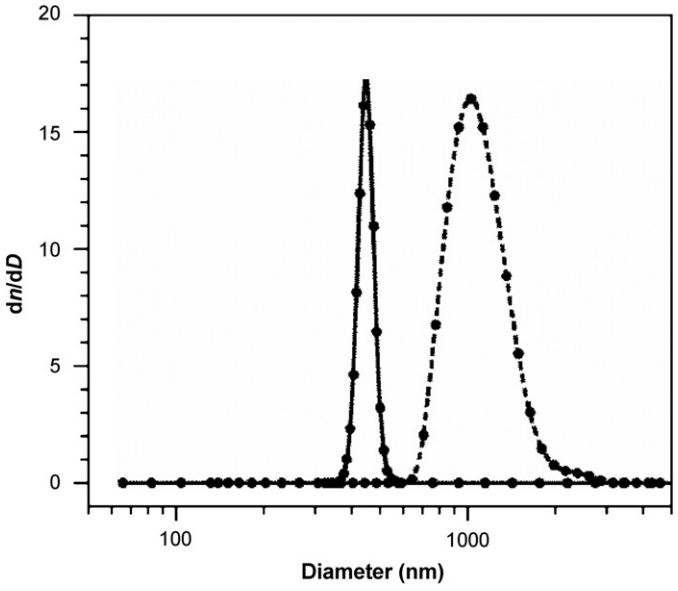

Fig. 2. Typical size distribution obtained by dynamic light scattering measurements for one of the studied system. Dashed line: primary emulsion; full line: nanocapsules. Organic phase = 0.2 g of PCL and 0.5 g of Miglyol 840 in 10 mL AcOEt, aqueous phase = 1 g of PVA in 40 mL water; emulsification with Ultra-Turrax at 8000 rpm for 10 min; 200 mL water added for the formation of nanocapsules.

3. Results and discussion

3.1. Example of nanocapsule preparation, control of the size and stability

The emulsion–diffusion process has been used successfully to prepare biodegradable nanocapsules in an efficient and reproducible manner. This process allowed the fabrication of stable aqueous dispersions of nanocapsules having controlled sizes in the range 100–500 nm. The control of the mean diameter of the nanocapsules was given by the choice of the composition of the organic phase and by the shear rate of the emulsification process. A simple geometrical relationship linked the mean diameter of the primary emulsion obtained at the first step and the final diameter of the nanocapsules obtained after the solvent diffusion step. For a clean process where neither coagulation nor droplet fragmentation took place during the solvent diffusion and evaporation steps, each individual emulsion droplet formed a nanocapsule. The removal of the organic solvent (ethyl acetate) decreased the volume of each droplet by a factor [oil + PCL]/[oil + PCL + AcOEt] given by the chemical composition of the organic phase. The decrease of the particle diameter was the third root of the decrease of the droplet volume:

$$\frac{D(\mathrm{NC})}{D(\mathrm{Em})} = \left[\frac{V_{\mathrm{oil}} + V_{\mathrm{PCL}}}{V_{\mathrm{oil}} + V_{\mathrm{PCL}} + V_{\mathrm{AcOEt}}}\right]^{1/3}. \quad (1)$$

Therefore, the primary emulsion having a z-average diameter $D(\mathrm{Em}) = 1100 \pm 50$ nm yielded a suspension of nanocapsules having a z-average diameter $D(\mathrm{NC}) = 425 \pm 5$ nm (Fig. 2). According to Eq. (1) and the recipe, the prediction was 447 nm.

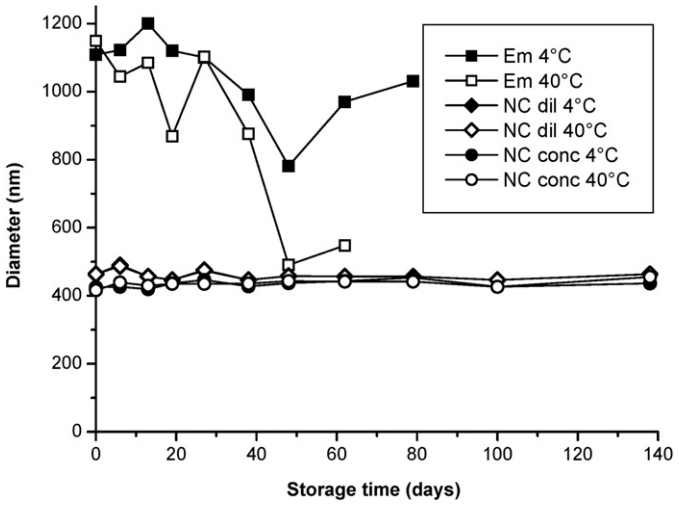

Fig. 3. Evolution of the size as a function of storage time at 4 and 40 °C for emulsion droplets (Em), nanocapsules in diluted (NC dil) and concentrated (NC conc) suspensions. Same recipe as in Fig. 2. The results at 20 °C not shown are close to those at 4 and 40 °C.

Equation (1) pertains to the mean diameter of the emulsion droplets, D(Em), and nanocapsules, D(NC), whatever the averaging process. It also pertains to each droplet, that is, to the full size distribution. Therefore, the size distribution of nanocapsules measured by dynamic light scattering can be predicted pretty well from the size distribution of the primary emulsion as measured by mean of the same technique (Fig. 2).

In order to use these nanocapsules in pharmaceutical field, the long time stability is of major importance. The particle diameter was measured against storage time at three temperatures, 4 °C, 20 °C and under ageing conditions at 40 °C, for emulsion droplets and their corresponding nanocapsules (Fig. 3). The sizes of nanocapsules were measured for suspensions stored before (diluted suspensions) and after (concentrated suspensions) the evaporation (i.e. respectively with or without organic solvent present in the external phase); every sample has been diluted to $\sim 10^{-4}$ immediately before each size measurement however, since accurate light scattering measurement required such a dilution.

The aqueous suspensions of nanocapsules were very stable during the studied lapse of time of 5 months as shown in Fig. 3. On the contrary, the primary emulsion was of poor stability. The measured droplet size started to decrease steeply after 20 days storage, possibly because creaming prevented a correct measurement; and it became impossible to obtain reproducible measurements after 60 days storage. It is worth noticing that such emulsions are quite peculiar since the droplets contain the polar organic solvent ethyl acetate and the aqueous phase is saturated with large amounts of the same solvent. Among the several disastrous processes [12] that may take place (coagulation, uncontrolled diffusion and evaporation of solvent), Ostwald ripening is the most likely. Ostwald ripening of emulsions is fast for oils having a high solubility in water. This mechanism causes the larger droplets of the size distribution to grow and the smaller to shrink. Very large droplets are not measured by the dynamic light scattering device when large amounts of small ones are present because the sample time is set short for a correct measurement of the small particles. Large particle are missed because their autocorrelation function decreases too slowly against time; they contribute to the scattering as an almost constant signal that is considered as background. In any case, the stability of the primary emulsion is enough for allowing the solvent diffusion step of the fabrication process without any stability trouble since the solvent diffusion step takes place in few milliseconds.

The good agreement between the predicted and experimental diameters of the nanocapsules and the stability results show that the solvent diffusion takes place in each independent emulsion droplet that can be considered as an isolated droplet leaking its content into the continuous phase.

3.2. *Effect of formulation parameters on nanocapsule formation*

Since the final size depends on the composition and emulsification process parameters of the primary emulsion, the influence of these parameters have been investigated in more details. Compared to classical oil-in-water emulsions, the present one has two specificities: it contains a polar organic solvent in its organic phase and the aqueous phase is saturated with 8.3% ethyl acetate. The influences of the classical formulation parameters have been studied in details on these particular emulsions made with very polar oil. The size of the nanocapsules was measured at the end of the full emulsion–diffusion process because it was easier experimentally. This size was related to the size of the primary emulsion as described above. Some results have been described in details in previous papers [7,11,13]. The influences of new parameters related to both the formulation and the mixing process are presently reported.

The influences of the different parameters are discussed with reference to the simple break-up mechanism of the oil liquid droplets caused by the shear stress, $\dot{\gamma}$, under laminar flow [14–16]. Droplet break-up is resisted by the interfacial tension, γ, between the oil and aqueous phases. This is described by the adimensional Capillary number, Ca, that compares the viscous stress that causes the droplet fragmentation and the restoring stress coming from surface forces [15]. For an oil-in-water emulsion the capillary number reads:

$$\mathrm{Ca} = \frac{\eta_{\mathrm{water}} \dot{\gamma} R}{\gamma}. \tag{2}$$

The droplets break-up when the capillary number exceeds a given value or, in other words, the radius R of the broken droplets is given by the limiting capillary number for droplet fragmentation. The capillary number is generally reported as a function of the viscosity ratio of the oil and aqueous phases $\eta_{\mathrm{oil}}/\eta_{\mathrm{water}}$, giving the classical Taylor master curve [14–16]. This scheme has been extended far beyond the original theory of Taylor to various types of flow and instrument geometries [17]. Given an emulsification process ($\dot{\gamma}$ is fixed), the relative viscosity of the organic and aqueous phases is therefore a well-known parameter that influences the size of the droplets.

Table 1
Influence of oil viscosity in the organic phase (oil + PCL + AcOEt) on nanocapsule mean size. PCL/oil = 1/2.5[a]

Oil type	Viscosity of oil at 20 °C (mPa s)	Mean size of NC (nm)
Miglyol 840	11	358 ± 5
Miglyol 812	30	483 ± 5
Miglyol 829	250	702 ± 10

[a] Experimental conditions: 1 g of PVA (80000 g/mol) in 40 mL aqueous phase (2.5% w/w), 0.2 g of PCL and 0.5 g of oil in organic phase (10 mL); emulsifying with Ultra-Turrax during 10 min at 8000 rpm.

Table 2
Influence of oil concentration in the organic phase (Miglyol 812 + PCL + AcOEt) on nanocapsule mean diameter[a]

Oil/polymer ratio	Mean size of NC (nm)
0.5/1	360 ± 10
1/1	351 ± 10
2/1	376 ± 10
2.5/1	483 ± 10

[a] Experimental conditions: 1 g of PVA (80000 g/mol) in 40 mL aqueous phase (2.5% w/w); 0.2 g of PCL in organic phase (10 mL); emulsifying with Ultra-Turrax during 10 min at 8000 rpm.

Table 3
Influence of concentration and molar mass of polymer (PCL) in the organic phase (oil + PCL + AcOEt) on nanocapsule mean size[a]

Mass of PCL (g) in 10 mL of organic phase	Molar mass of PCL (g/mol)	Mean size of NC (nm)
0.1	80 000	465 ± 5
0.2		483 ± 5
0.4		457 ± 5
0.8		470 ± 5
0.2	14 000	456 ± 5
	65 000	420 ± 5
	80 000	483 ± 5

[a] Experimental conditions: 1 g of PVA (80000 g/mol) in 40 mL aqueous phase (2.5% w/w); 0.5 g of Miglyol 812 and varying amounts of PCL in organic phase (10 mL); emulsifying with Ultra-Turrax during 10 min at 8000 rpm.

The oil viscosity (Table 1) affected the droplet size according to expectations: the larger was the oil viscosity, the larger was the droplet diameter. The viscosity ratio of the oil and aqueous phases was indeed in the domain $\eta_{oil}/\eta_{water} > 1$ of the Taylor curve where the size increases as a function of this ratio. The variation of the nanocapsule diameter was moderate however, which showed that the system was close to the minimum of the Taylor curve where the smaller diameter was obtained.

The nanocapsule diameter slightly increased with the oil concentration (Table 2). Such a variation could be rationalized again with the help of the Taylor curve since an increase of the oil content in the organic phase made it more viscous. Here again, the variation of diameter was very weak, showing that the experimental conditions were close to the minimum capillary number.

The concentration and molar mass of the PCL polymer did not influence the overall size of the nanocapsules (Table 3) in the studied range polymer molar masses (14 000, 65 000 or 80 000 g/mol) and concentrations from 10 to 100 g/L in organic phase. Thickening the organic phase by the PCL polymer has no significant effect as previously mentioned. The emulsification conditions close to the minimum capillary number is presumably the origin of such insensitivity to these parameters. This later observation has an important practical implication for the preparation of nanocapsules. Indeed, it was possible to increase the polymer content of the organic phase keeping the particle size constant, therefore giving an easy way to increase the polymer membrane thickness of the nanocapsules at constant overall diameter.

Table 4
Influence of concentration and molar mass of stabilizer (PVA) in the aqueous phase on nanocapsule NC mean size[a]

Mass of PVA (g) in 40 mL of aqueous phase	Molar mass of PVA (g/mol)	Mean size of NC (nm)
0.2	88 000	365 ± 5
0.5		383 ± 5
1		483 ± 5
1.5		1247 ± 50
1	31 000	456 ± 5
	88 000	483 ± 5

[a] Experimental conditions: 0.2 g of PCL (80000 g/mol) and 0.5 g of Miglyol 812 in organic phase (10 mL); emulsifying with Ultra-Turrax during 10 min at 8000 rpm.

The global size was not influenced by molar mass of the PVA stabilizer but it depended on its concentration: the larger was the PVA concentration, the larger was the nanocapsule size (Table 4).

A higher concentration (or molar mass) of PVA stabilizer makes the aqueous phase more viscous, therefore increasing the mean nanocapsule diameter at nearly constant capillary number. The increase of nanoparticle size caused by increasing the PVA concentrations has already been observed in several instances [18,19].

Regarding the stirring stage, the nanocapsule diameter depends on several parameters according to common knowledge. The nanocapsule size was smaller upon increasing the stirring speed and/or time [13]. Smaller nanocapsules were produced when the stirring process was changed from shear mode (Ultra-Turrax) to cavitation mode (ultrasound dispersing apparatus VibraCell 75042 from Bioblock), keeping the same experimental conditions and emulsification time. Therefore, it is possible to decrease the nanocapsule size by a suitable choice of the emulsification technology.

Finally, the influence of the water addition mode during the second step of the process (the dilution) was investigated. The volume of water added to the emulsion was an essential parameter regarding the control of nanocapsule size since an insufficient volume of water does not allow the full release of ethyl acetate out from the emulsion droplets. Partial removal of ethyl acetate is reported in the following section. In cases where the total volume of added water is larger than the minimum volume corresponding to the solubility of the full ethyl acetate in the aqueous phase, the mode of addition (one-shot

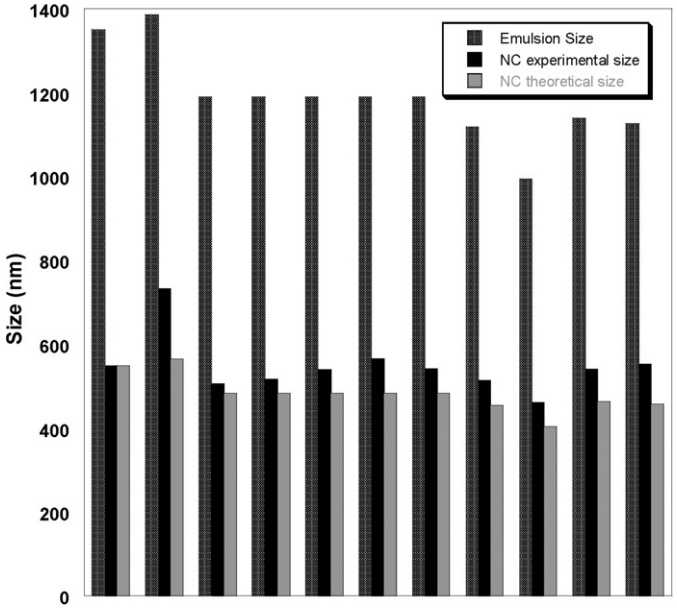

Fig. 4. Test of the reproducibility and comparison between experimental and calculated nanocapsule sizes for different experiment performed in the same conditions. Organic phase = 0.2 g of PCL and 0.5 g of Miglyol 840 in 10 mL AcOEt, aqueous phase = 1 g of PVA in 40 mL water; emulsification with Ultra-Turrax at 8000 rpm for 10 min; 200 mL water added for the formation of nanocapsules. The sizes of the primary emulsion are also reported on this graph.

or drop-wise) and the rate of water addition were not sensitive parameters.

The nanocapsule size is related to the emulsion droplet diameter by mean of Eq. (1) when all solvent (AcOEt) has been removed from the droplets after the water addition and solvent evaporation. The results for several identical experiments represented in Fig. 4 show the reproducibility of the sizes. Measured sizes are very close to the calculated ones. But the experimental nanocapsule sizes were systematically slightly higher than the calculated one. Presumably the measurements of the primary emulsion size were not perfectly accurate owing to the difficulties of correct dilution for performing dynamic light scattering. Indeed, the emulsions should have been diluted with water saturated with ethyl acetate, which was quite unstable with respect to demixion. Good reproducibility was achieved by means of dilution with a slightly undersaturated solution of ethyl acetate in water; therefore the size of the primary emulsion was slightly underestimated. Finally, there was no residual solvent in the nanocapsules since no trace of ethyl acetate could be detected in the final concentrated suspensions by gas chromatography measurements.

By varying these different parameters, we could prepare aqueous suspensions of well-defined nanocapsules having diameters ranging between 250 nm to 5 μm and having narrow size distributions. Most of the formulations led to similar nanometric sizes because the capillary number was close to the flat minimum of the Taylor curve where the sensitivity to formulation parameters was the lowest. Larger capsules up 5 μm diameter could be prepared by lowering the shear rate of the Ultra-Turrax.

3.3. Internal structure of the nanocapsules

The expected nanocapsule morphology was made of an oil core surrounded by a polymer shell. It was quite a difficult task to obtain direct experimental evidence of the core–shell morphology of nanocapsules. Experimental data reported so far were better strong indication giving support to such morphology than definite proof. They were obtained by means of indirect measurements such as observations of the improved stability and the slower release rate of encapsulated materials [13]. Transmission electron microscopy pictures could provide additional support [12,13,20] but not definite proof because this was strongly dependent on the staining processes that was necessary to reveal the polymer shell. Because the nanocapsules are very small, the thickness of the polymer shell is necessarily much smaller. The electron microscopy techniques that are successful for demonstrating the capsule morphology of microcapsules do not work in the present case. Indeed the typical size of microcapsules is 10–100 μm and the polymer membrane is few micrometers thick. Therefore, the thick polymer membrane is easily observed and it resists sampling processes of electron microscopy because of it has high enough mechanical strength. The scale of nanocapsules is a factor of one thousand smaller, so that the polymer membrane thickness is of the order 1–10 nm. The polymer membrane is therefore very soft and easy to crack under the constraints of sampling processes (deposition on the surface of the grid and drying, observation under high vacuum). A last difficulty is the small thickness that is of the same order of magnitude as the stabilizing layer of adsorbed PVA. This was quite difficult to distinguish the PCL shell and the adsorbed PVA, especially after a staining process.

There were several adverse effects of the presence of PVA in the samples when the suspensions are observed by means of transmission electron microscopy. “Direct” observations consisted in diluting the suspension to 10^{-4} and drying a thin film of it deposited on the microscope grid. In addition to the typical spherical particles corresponding to the expected nanocapsules, small lumps of irregular shape were observed in the pictures. These supplementary particles were made of pure PVA. The phosphotungstic acid staining agent stained the PVA particles and the adsorbed PVA; these dark areas obscured the observation of the remaining parts of the picture. In particular, the adsorbed PVA appeared as a hallo around the particles. The excess PVA was eliminated by centrifugation. This purification of the aqueous phase was successful when using Miglyol 829 as oil in combination with PCL because the densities of both materials were higher than water, allowing the sedimentation of the particles in the ultracentrifuge. On the contrary for Miglyol grades of density lower than water, the density of their mixtures with PCL was close to water and the separation by centrifugation was unsuccessful. The density of PCL is 1.145 g/cm^3 and those of Miglyol 812, 829 and 840 are 0.945, 1.010, 0.915 g/cm^3, respectively [9]. Thus, the suspension was centrifuged at 15 000 rpm for 1 h with a Beckman–Coulter Optima MAX-E ultracentrifuge; the supernatant was removed and the suspension was diluted to 10^{-4} with pure water.

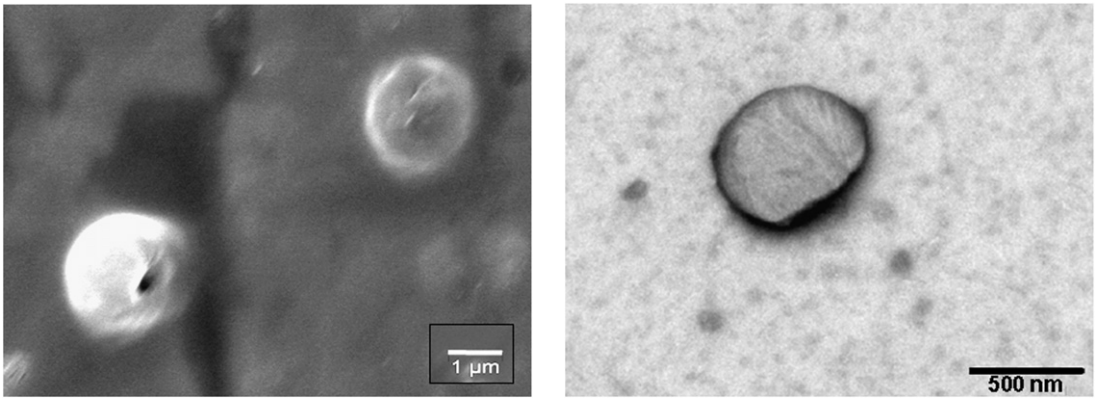

(a) (b)

Fig. 5. (a) SEM image of nanocapsules. (b) TEM image of an isolated nanocapsule obtained in the presence of the negative staining agent phosphotungstic acid. Organic phase = 0.2 g of PCL and 0.5 g of Miglyol 829 in 10 mL AcOEt, aqueous phase = 1 g of PVA in 40 mL water; emulsification with Ultra-Turrax at 8000 rpm for 10 min; 200 mL water added for the formation of nanocapsules.

Scanning and transmission electron microscopy allowed the observation of the particles and confirmed the nanocapsule size obtained by light scattering. Fig. 5 shows images of nanocapsules with different diameter (corresponding to different experimental conditions). In both cases, well-defined particles having spherical form were observed. The diameters measured on the pictures were in good agreement with those determined by light scattering analysis.

The visualization of the thin polymeric membrane was made by transmission electron microscopy after freeze-fracture sampling. The theoretical thickness of the polymeric membrane can be estimated from the experimental diameter of the nanocapsule, D, and the composition of the organic phase as:

$$h = \frac{D}{2}\left[1 - \left(\frac{V_{\text{oil}}}{V_{\text{oil}} + V_{\text{PCL}}}\right)^{1/3}\right]. \tag{3}$$

The underlying assumptions are the full phase separation of the polymer and oil inside the particles and a homogeneous thickness of the polymer shell. For instance, the theoretical polymeric membrane thickness is 35 nm for nanocapsules of diameter 457 nm which were obtained by using 0.4 g of PCL (80 000 g/mol) and 0.5 g of Miglyol 812 in 10 mL of organic phase 0.5 g of PVA (88 000 g/mol) in 40 mL of aqueous phase.

Quenching the aqueous dispersion turned the particles into their solid state, allowing their fracture without deformation. Replicas of the fractured surface were observed by means of TEM. Either fracture took place in the aqueous solidified solvent, keeping the particles intact, or the particles were broken into pieces that revealed their internal structure (Fig. 6).

The TEM image in Fig. 6a corresponds to a freeze-fracture process that kept the entire nanocapsule whereas the second image in Fig. 6b shows a piece of broken particle that is compatible with the presence of a hollow structure. In this latter case, the membrane thickness could be estimated at the edge of the membrane fragment around 30 nm, which was in good agreement with the calculated thickness. Nevertheless, the determination of membrane thickness using freeze-fracture microscopy was very difficult because of the small number of nanocapsules

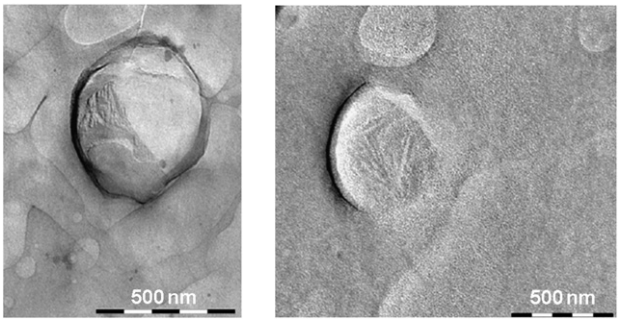

(a) (b)

Fig. 6. TEM analysis of the nanocapsules prepared by freeze-fracture. Same type of sample as in Fig. 5.

that have been broken and leaved in a favorable position for an observation. Such a lack of data of statistical significance does not allow a definite conclusion regarding the average thickness. It is necessary to confirm these experimental data by further investigations that give a satisfactory statistical average such as the small angle neutron scattering experiments to be reported soon. Such experiments making use of deuterium-labeled materials have been successful for investigating the internal structure of core–shell latexes and more complex heterogeneous systems made of emulsion polymers [21–23].

As a summary, this part of the study on the internal structure has shown that the morphology of nanocapsules was of the core–shell type and that the polymer membrane thickness was indeed in the expected range.

3.4. *Nanocapsule formation during the solvent diffusion stage*

In order to get better understanding on the nanocapsule formation, different intermediate states taking place during the dilution step have been investigated. Two types of experiments have been designed: (i) a step-by-step extraction of ethyl acetate out of the droplet by means of discrete dilutions that allowed partial diffusion of ethyl acetate; (ii) tentative time-resolved experiments using a stopped-flow fast mixing device.

3.4.1. "Step by Step" study of nanocapsule formation

Partial diffusion of ethyl acetate out of the emulsion droplets have been performed by addition of the suitable amounts of water. Investigation of these "quenched" intermediate states allowed looking for possible accidents or transitions that could take place during the solvent diffusion process. The step-wise extraction of the solvent mimics a very slow process that would consist in consecutive equilibrium states. The primary emulsion was prepared and divided into several batches that were diluted with different amounts of water in order to cause the diffusion of a fraction of the AcOEt out from the droplets into external phase. The resulting shrinkage of the droplets was measured by dynamic light scattering. The droplet diameter could be calculated from the residual volume of ethyl acetate inside the droplets ($V_{\mathrm{AcOEt}}(\mathrm{res})$) and the parameters of the primary emulsion ($D(\mathrm{init})$ and $V_{\mathrm{AcOEt}}(\mathrm{init})$) by means of equation:

$$\frac{D}{D(\mathrm{init})} = \left[\frac{V_{\mathrm{oil}} + V_{\mathrm{PCL}} + V_{\mathrm{AcOEt}}(\mathrm{res})}{V_{\mathrm{oil}} + V_{\mathrm{PCL}} + V_{\mathrm{AcOEt}}(\mathrm{init})}\right]^{1/3}. \tag{4}$$

As first approximation, the volumes of water were calculated by assuming that the external phase was always saturated in organic solvent. Distilled water solubilizes 8.3 wt% of AcOEt at saturation, corresponding to a volume fraction of ethyl acetate $x_{\mathrm{sat}} = 9.1\%$. Accordingly, the amount of ethyl acetate remaining inside the droplets and the droplet diameter were calculated from Eq. (4) and

$$\frac{V_{\mathrm{AcOEt}}(\mathrm{res})}{V_{\mathrm{AcOEt}}(\mathrm{init})} = 1 - \frac{x_{\mathrm{sat}} V_{\mathrm{added\ water}}}{V_{\mathrm{AcOEt}}(\mathrm{init})}. \tag{5}$$

Another way for proceeding a partial diffusion of ethyl acetate out from the particles was a dilution with a fixed volume of water partially saturated with a volume fraction x_{AcOEt} of ethyl acetate. According to this later process, the amount of ethyl acetate leaving the particle was approximately the amount required for establishing the saturation of the aqueous phase. The amount of ethyl acetate remaining inside the droplets was calculated from equation

$$\frac{V_{\mathrm{AcOEt}}(\mathrm{res})}{V_{\mathrm{AcOEt}}(\mathrm{init})} = 1 - \frac{(x_{\mathrm{sat}} - x_{\mathrm{AcOEt}}) V_{\mathrm{added\ water}}}{V_{\mathrm{AcOEt}}(\mathrm{init})}. \tag{6}$$

Note that Eq. (6) reduces to Eq. (5) when $x_{\mathrm{AcOEt}} = 0$ (dilution with pure water).

According to these two protocols, the droplet sizes were measured at the intermediate states defined by the residual amount of ethyl acetate inside the particles (Fig. 7). It was observed that the two methods of solvent diffusion out from the droplet were equivalent. The predictions of Eqs. (4), (5) and (6) showed excellent agreement with experiments at the beginning of solvent diffusion. The predictions were slightly but significantly lower than the experimental diameters at high shrinkages (Fig. 7). Therefore, the amount of ethyl acetate that left the droplets was lower than the amount required for establishing again the saturation of the aqueous phase. Ethyl acetate was therefore partitioned between the droplets and the aqueous phase. A more elaborate modeling of the droplets shrinkage according to partition equilibrium of the ethyl acetate can be devised using a single partition equilibrium described by a mass-action law (Eq. (7)). One underlying assumption is the validity of a mass-action law, that is, ideal solution behavior. The second assumption considers that the "organic phase" remains identical throughout the full depletion of ethyl acetate, starting from the initial emulsion containing ~90% AcOEt and ending with a nanocapsule droplet made of a diphasic medium containing the oil and PCL. Full calculations are reported in Appendix A for the two dilution processes either with increasing amounts of pure water or with a fixed volume of water containing increasing amounts of ethyl acetate,

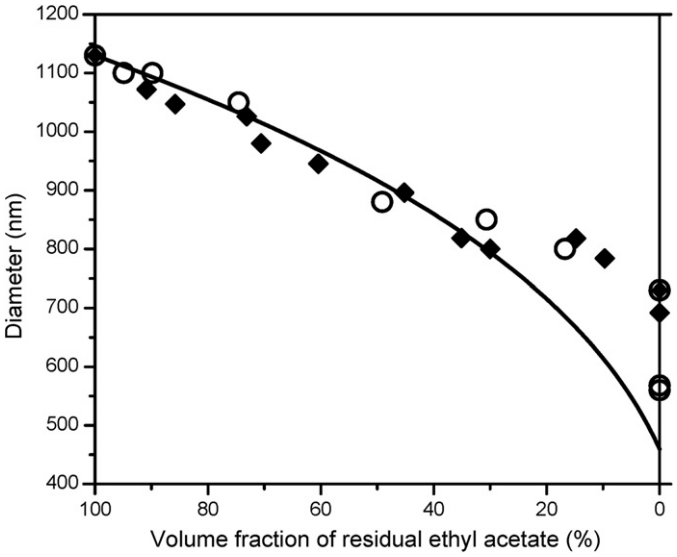

Fig. 7. Size evolution according to the fraction of ethyl acetate contained in nanocapsules as calculated with the approximate Eqs. (5) and (6). (●) Dilution with increasing amounts of pure water; (◆) Dilution with a fixed volume (25 cm^3 into 10 cm^3 initial emulsion volume) of water partially saturated with ethyl acetate; Solid line: Prediction of the combined Eqs. (4), (5) and (6). 100% AcOEt = emulsion state: 0% AcOEt = nanocapsule state.

$$\frac{[\mathrm{AcOEt}]_{\mathrm{oil}}}{[\mathrm{AcOEt}]_{\mathrm{water}}} = K. \tag{7}$$

Expressing the concentrations as volume of AcOEt per unit volume of phase instead of the classical mol/volume unit, the concentrations are identical to the volume fractions $x_{\mathrm{AcOEt}}(\mathrm{oil})$ and $x_{\mathrm{AcOEt}}(\mathrm{water})$. The equilibrium of ethyl acetate between a saturated aqueous phase ($x_{\mathrm{sat}} = 9.1\%$) and pure ethyl acetate reads accordingly

$$K = \frac{x_{\mathrm{AcOEt}}(\mathrm{oil})}{x_{\mathrm{AcOEt}}(\mathrm{water})} = \frac{1}{0.091} = 10.7. \tag{8}$$

Taking this value of K, the variation of the measured diameter could be accurately modeled for the two dilution processes without the help of any fitting parameter (Fig. 8). The approximate calculation described by Eqs. (5) and (6) departed from the experimental data for both dilution processes when the fraction of residual AcOEt was below 30%.

The successful modeling of the stepwise extraction of AcOEt shows that such diffusion of AcOEt out from the droplets took place as a continuous process. There is no accident (discontinuity) that would reveal a transition from homogeneous droplets to heterogeneous capsules. The simple

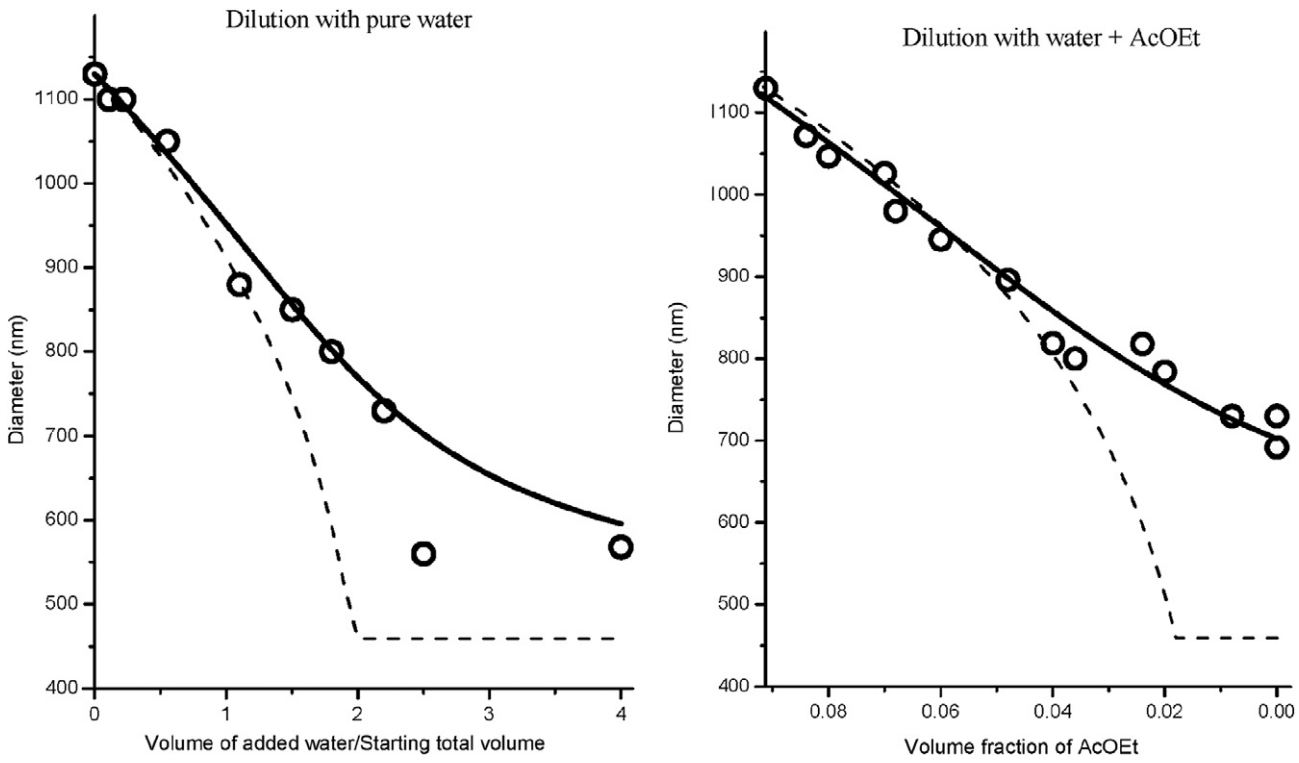

(a) (b)

Fig. 8. Size evolution with respect to the amounts added materials according to the two dilution processes. (a) Dilution with increasing amounts of pure water; (b) dilution with a fixed volume (25 cm^3 into 10 cm^3 initial emulsion volume) of water partially saturated with ethyl acetate; (○) experimental; Solid lines: prediction of the modeling with AcOEt partition using $K = 10.7$; Dashed lines: approximate prediction of the combined Eqs. (4), (5) and (6).

geometrical model is an acceptable approximation at low deswelling rates. It should be noticed that the final diameter of nanocapsules obtained at the end of the full process (Fig. 2) was smaller of that measured after the dilution with the maximum amount of pure water because the residual ethyl acetate inside the particles has been removed during the final evaporation step, giving nanocapsules free of ethyl acetate.

3.4.2. *Duration of the solvent diffusion step*

Since the solvent diffusion takes place quite fast after the one shot addition of water, it has been attempted to measure the duration of this stage by means of time-resolved experiments after fast mixing using the stopped-flow technique. The stopped-flow apparatus allows to monitor the process by either turbidity (absorbance) or fluorescence measurements after mixing two solutions in a very short time (Fig. 9). The stopped-flow principle of operation allows small volumes of solutions to be driven from high-performance syringes to a high efficiency mixer just before passing into a measurement flow cell. As the solutions flow through, steady state equilibrium is established and the resultant solution is only a few milliseconds old as it passes through the cell. The mixed solution then passes into a stopping syringe which stops the flow instantaneously and traps the resultant solution in the flow cell. The kinetics was followed by absorbance measurements. The mixing time is 10 ms with used apparatus [24]. The two separated syringes were filled with the emulsion and distilled water at the beginning. They were mixed for in situ formation of nanocapsules.

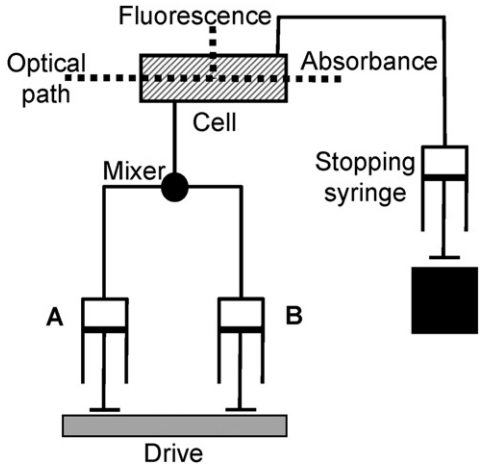

Fig. 9. Scheme of the stopped-flow apparatus.

The turbidity of the mixed sample was recorded as a function of time (Fig. 10).

The only signal corresponding to the final state could be observed (Fig. 10) and no evolution between initial and final state could be detected. The turbidity indeed corresponded to that arising from nanocapsules. The dilution of the starting emulsion with water saturated with ethyl acetate allowed a dilution of the emulsion without diffusion of ethyl acetate out from the droplets. In that case, the recording was corresponding to the emulsion that had a much higher absorbance than nanocapsules. It was concluded that the diffusion step was too

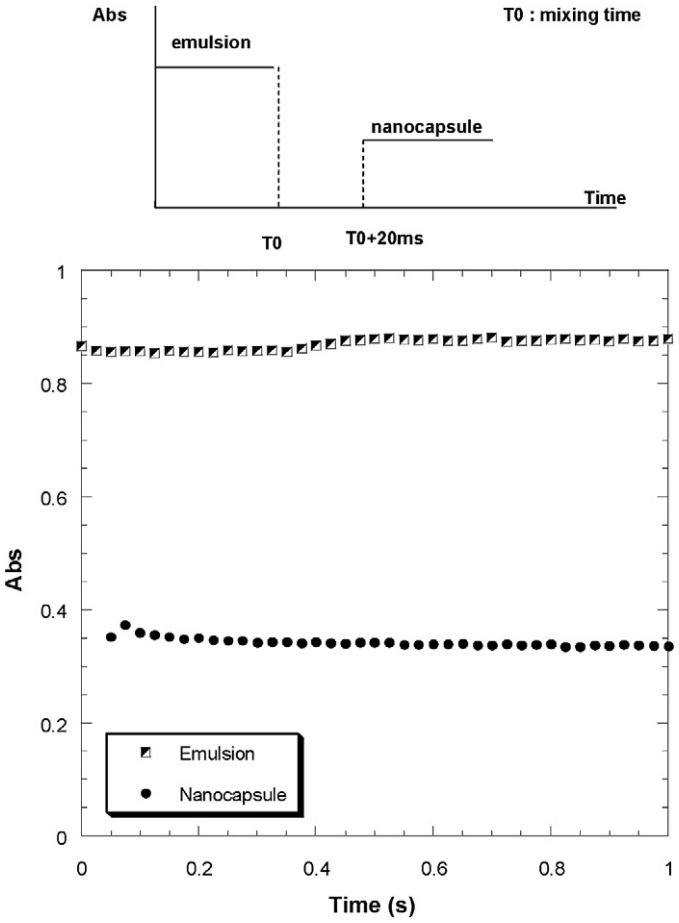

Fig. 10. Absorbance during a kinetic measurements of solvent diffusion step from emulsion droplets to nanocapsule by stopped-flow apparatus: (top) schematic representation, (bottom) after mixing of emulsion and distilled water, the experimental signal corresponding to nanocapsule was measured. The signal of the starting emulsion was also recorded for comparison.

fast for being detected with the help of this experimental set-up. Recording of the absorbance started after a dead time of 20 ms corresponding to the acquisition time of the spectrometer. As a consequence, the actual duration of diffusion step could not be evaluated. 20 ms is the upper limit of this time. It was not possible to slow down enough the diffusion time by using concentrated solutions of PCL of high molar mass as organic phase. Park could observe the diffusion of solvent out of microspheres of poly(lactic acid) made of polymer having high molar mass [25]. The measurements by Park were successful because microspheres were investigated instead of nanoparticles. The diffusion path was larger and the characteristic time longer. The very short diffusion time is a consequence of the small droplet size. An order of magnitude of the expected diffusion time is estimated as the time required for diffusion over the radius of the starting emulsion. Thus, $t = R^2/D$ gives 0.1 ms diffusion time for a radius $R = 500$ nm and a diffusion coefficient of the small organic molecule AcOEt $D = 2 \times 10^{-9}$ m^2/s. The possible formation of the polymer shell during the diffusion process might have built a barrier preventing the leakage of ethyl acetate. Such a phenomenon obviously did not occur.

4. Conclusions

The preparation of well-defined nanocapsules has been successfully carried out using the two stages "emulsion–diffusion" process. It has been shown that the size of the final nanocapsules was related to the chemical composition of the organic phase and the size of primary emulsion by a simple geometrical relationship. As a consequence, most of the properties of the nanocapsules were decided at the emulsification step. Different systems have been obtained by changing experimental parameter during the emulsion step. Several formulation parameters were not sensitive because the viscosities of water and organic phase were similar, placing the primary emulsion at the flat minimum of the Taylor curve relating the capillary number to the viscosity ratio. The final nanocapsule properties depended mainly on the oil-to-polymer ratio that fixed the shell thickness and the mixing parameters (mixing device, shear rate) that fixed the size of the primary emulsion. The vesicular nature of nanocapsules has been clearly shown by freeze fracture microscopy. The thickness of the polymeric membrane was close to the calculated one.

Acknowledgments

We are grateful to Marie-Geneviève Blanchin and Andrei Popescu (Laboratoire de Physique de la Matière Condensée et des Nanostructures, UMR 5586 CNRS, University of Lyon) for their help in electron microscopy observations.

Appendix A

The diameter of the droplets was calculated from Eq. (4) relating the diameter of the partially de-swollen droplets to the diameter of the starting emulsion and the amount of residual ethyl acetate contained inside the droplets. This later quantity was calculated as follows from the partition coefficient (Eq. (7)) and the balance of AcOEt according to the type of dilution process. All amounts are given as volumes in the following equations; concentrations are therefore volume fractions.

The volume of AcOEt, $V_{\mathrm{AcOEt}}(\mathrm{total})$, is constant and the volume of water increases according to the added volume $V_{\mathrm{water}}(\mathrm{added})$.

The partition equilibrium is

$$K = \frac{x_{\mathrm{AcOEt}}(\mathrm{oil})}{x_{\mathrm{AcOEt}}(\mathrm{water})} = \frac{V_{\mathrm{AcOEt}}(\mathrm{oil})}{V_{\mathrm{AcOEt}}(\mathrm{water})} \frac{(V_{\mathrm{water}} + V_{\mathrm{AcOEt}}(\mathrm{water}))}{(V_{\mathrm{oil}} + V_{\mathrm{PCL}} + V_{\mathrm{AcOEt}}(\mathrm{oil}))}. \quad (A.1)$$

A.1. Dilution with increasing volumes of pure water

The total volume of water is

$$V_{\mathrm{water}} = V_{\mathrm{water}}(\mathrm{initial}) + V_{\mathrm{water}}(\mathrm{added}). \quad (A.2.1)$$

Ethyl acetate is found in both water and oil phases; its amount is the sum of the starting volumes introduced in the oil phase, $V_{\mathrm{AcOEt}}(\mathrm{oil\ initial})$ and in the water phase, $V_{\mathrm{AcOEt}}(\mathrm{water\ initial})$

$= x_{\text{sat}} \times V_{\text{water}}(\text{initial})$. The volume balance of AcOEt writes

$$V_{\text{AcOEt}}(\text{total}) = V_{\text{AcOEt}}(\text{oil initial}) + V_{\text{AcOEt}}(\text{water initial}) = V_{\text{AcOEt}}(\text{oil}) + V_{\text{AcOEt}}(\text{water}). \quad (A.3.1)$$

A.2. Dilution with fixed volumes of water containing decreasing amounts of ethyl acetate

The total volume of water is

$$V_{\text{water}} = V_{\text{water}}(\text{initial}) + (1 - x_{\text{AcOEt}})V(\text{added}). \quad (A.2.2)$$

The amount of ethyl acetate is the sum of the starting volumes introduced in the oil and water phases, and that added in the partially saturated aqueous phase used for the dilution. The volume balance of AcOEt writes

$$V_{\text{AcOEt}}(\text{total}) = V_{\text{AcOEt}}(\text{oil initial}) + V_{\text{AcOEt}}(\text{water initial}) + x_{\text{AcOEt}}V(\text{added}). \quad (A.3.2)$$

The set of Eqs. (A.1)–(A.3) is solved for $x = V_{\text{AcOEt}}(\text{oil})$ which allows calculating the diameter as a function of added water. Simple algebra gives the following second degree equation of the form $ax^2 + bx + c = 0$:

$$(K-1)x^2 + \left[V_{\text{water}} + K(V_{\text{oil}} + V_{\text{PCL}}) - (K-1)V_{\text{AcOEt}}(\text{total})\right]x - K V_{\text{AcOEt}}(\text{total})(V_{\text{oil}} + V_{\text{PCL}}) = 0. \quad (A.4)$$

Its analytical solution is

$$x = V_{\text{AcOEt}}(\text{oil}) = \frac{-b + \sqrt{b^2 - 4ac}}{2a}.$$

References

[1] D. Moinard-Checot, Y. Chevalier, S. Briançon, H. Fessi, S. Guinebretière, J. Nanosci. Nanotechnol. 6 (2006) 2664–2681.

[2] S. Benita (Ed.), Microencapsulation. Methods and Industrial Applications, Marcel Dekker, New York, 1996.

[3] P. Couvreur, L. Grislain, V. Lenaerts, F. Brasseur, P. Guiot, A. Biernacki, in: P. Guiot, P. Couvreur (Eds.), Polymeric Nanoparticles and Microspheres, CRC Press, Boca Raton, FL, 1986, pp. 27–93.

[4] R. Gref, Y. Minamitake, M.T. Peracchia, V. Trubetskoy, V. Torchilin, R. Langer, Science 263 (1994) 1600–1603.

[5] D. Quintanar-Guerrero, H. Fessi, É. Doelker, É. Allémann, Procédé de préparation de nanocapsules de type vésiculaire, utilisables notamment comme vecteurs colloïdaux de principes actifs pharmaceutiques ou autres, Fr. Pat. 2 766 368 (1997); Eur. Pat. 1 003 488 (1998); US Pat. 6 884 438 (2005).

[6] D. Quintanar-Guerrero, É. Allémann, H. Fessi, É. Doelker, Int. J. Pharm. 143 (1996) 133–141.

[7] D. Quintanar-Guerrero, É. Allémann, É. Doelker, H. Fessi, Colloid Polym. Sci. 275 (1997) 640–647.

[8] D. Quintanar-Guerrero, É. Allémann, É. Doelker, H. Fessi, Pharm. Res. 15 (1998) 1056–1062.

[9] Miglyol Product information, Condea Chemie GmbH.

[10] H. Stephen, T. Stephen, in: Solubilities of Inorganic and Organic Compounds, vol. 1, Pergamon Press, Oxford, 1963, Part 1.

[11] S. Guinebretière, Nanocapsules par émulsion diffusion de solvant: Obtention, caractérisation et mécanisme de formation, Ph.D. thesis, University Lyon 1, 2001.

[12] P. Walstra, P. Becher (Eds.), Encyclodedia of Emulsion Technology, vol. 4, Marcel Dekker, New York, 1996, pp. 1–62.

[13] S. Guinebretière, S. Briançon, J. Lieto, C. Mayer, H. Fessi, Drug Dev. Res. 57 (2002) 18–33.

[14] G.I. Taylor, Proc. Royal Soc. A 146 (1934) 501–523.

[15] J.M. Rallison, Ann. Rev. Fluid Mech. 16 (1984) 45–66.

[16] B.J. Briscoe, C.J. Lawrence, W.G.P. Mietus, Adv. Colloid Interface Sci. 81 (1999) 1–17.

[17] B.J. Bentley, L.G. Leal, J. Fluid Mech. 167 (1986) 241–283.

[18] H. Murakami, Y. Kawashima, T. Niwa, T. Hino, H. Takeuchi, M. Kobayashi, Int. J. Pharm. 149 (1997) 43–49.

[19] A. Loxley, B. Vincent, J. Colloid Interface Sci. 208 (1998) 49–62.

[20] S. Guinebretière, S. Briançon, H. Fessi, V.S. Theodorescu, M.-G. Blanchin, Mater. Sci. Eng. C 21 (2002) 137–142.

[21] R.H. Ottewill, S.J. Cole, J.A. Waters, Macromol. Symp. 92 (1995) 97–107.

[22] N. Dingenouts, J. Bolze, D. Pötschke, M. Ballauff, Adv. Polym. Sci. 144 (1999) 1–47.

[23] Y. Chevalier, Trend Polym. Sci. 4 (1996) 197–203.

[24] L. Beney, I. Martínez de Marañón, P.A. Maréchal, S. Moundanga, P. Gervais, Biochem. Eng. J. 9 (2001) 205–210.

[25] T.G. Park, J. Controlled Release 30 (1994) 161–173.